














Article

Flexible Sample Environments for the Investigation of Soft Matter at the European Spallation Source: Part I—The In Situ SANS/DLS Setup

Andreas Josef Schmid ¹, Lars Wiehemeier ¹, Sebastian Jaksch ², Harald Schneider ³, Arno Hiess ³,
Torsten Bögershausen ³, Tobias Widmann ⁴, Julija Reitenbach ⁴, Lucas P. Kreuzer ⁴,
Matthias Kühnhammer ⁵, Oliver Löhmann ^{3,5}, Georg Brandl ², Henrich Frielinghaus ²,
Peter Müller-Buschbaum ^{4,6}, Regine von Klitzing ⁵ and Thomas Hellweg ^{1,*}

- ¹ Physikalische und Biophysikalische Chemie, Fakultät f. Chemie, Universität Bielefeld, Universitätsstr. 25, 33615 Bielefeld, Germany; andreas.josef.schmid@rwth-aachen.de (A.J.S.); lars.wiehemeier@uni-bielefeld.de (L.W.)
 - ² Jülich Centre for Neutron Science JCNS at Heinz Maier-Leibnitz Zentrum (MLZ), Forschungszentrum Jülich GmbH, Lichtenbergstr. 1, 85748 Garching, Germany; s.jaksch@fz-juelich.de (S.J.); g.brandl@fz-juelich.de (G.B.); h.frielinghaus@fz-juelich.de (H.F.)
 - ³ European Spallation Source ERIC, P.O. Box 176, 221 00 Lund, Sweden; harald.schneider@ess.eu (H.S.); arno.hiess@ess.eu (A.H.); torsten.bogershausen@ess.se (T.B.); loehmann@fkp.tu-darmstadt.de (O.L.)
 - ⁴ Lehrstuhl f. funktionelle Materialien, Physik Department, Technische Universität München, James-Franck-Str. 1, 85748 Garching, Germany; Tobias.widmann@ph.tum.de (T.W.); julija.reitenbach@ph.tum.de (J.R.); lucas.kreuzer@ph.tum.de (L.P.K.); muellerb@ph.tum.de (P.M.-B.)
 - ⁵ Institut für Physik Kondensierter Materie, Technische Universität Darmstadt, Hochschulstr. 8, 64289 Darmstadt, Germany; kuehnhammer@fkp.tu-darmstadt.de (M.K.); klitzing@smi.tu-darmstadt.de (R.v.K.)
 - ⁶ Heinz Maier-Leibnitz Zentrum (MLZ), Technische Universität München, Lichtenbergstr. 1, 85748 Garching, Germany
- * Correspondence: thomas.hellweg@uni-bielefeld.de



Citation: Schmid, A.J.; Wiehemeier, L.; Jaksch, S.; Schneider, H.; Hiess, A.; Bögershausen, T.; Widmann, T.; Reitenbach, J.; Kreuzer, L.P.; Kühnhammer, M.; et al. Flexible Sample Environments for the Investigation of Soft Matter at the European Spallation Source: Part I—The In Situ SANS/DLS Setup. *Appl. Sci.* **2021**, *11*, 4089. <https://doi.org/10.3390/app11094089>

Academic Editor: Richard Yong
Qing Fu

Received: 12 April 2021
Accepted: 27 April 2021
Published: 29 April 2021

Publisher's Note: MDPI stays neutral with regard to jurisdictional claims in published maps and institutional affiliations.



Copyright: © 2021 by the authors. Licensee MDPI, Basel, Switzerland. This article is an open access article distributed under the terms and conditions of the Creative Commons Attribution (CC BY) license (<https://creativecommons.org/licenses/by/4.0/>).

Abstract: As part of the development of the new European Spallation Source (ESS) in Lund (Sweden), which will provide the most brilliant neutron beams worldwide, it is necessary to provide different sample environments with which the potential of the new source can be exploited as soon as possible from the start of operation. The overarching goal of the project is to reduce the downtimes of the instruments related to changing the sample environment by developing plug and play sample environments for different soft matter samples using the same general carrier platform and also providing full software integration and control by just using unified connectors. In the present article, as a part of this endeavor, the sample environment for in situ SANS and dynamic light scattering measurements is introduced.

Keywords: dynamic light scattering; small angle neutron scattering; instrumentation; microgels

1. Introduction

The new European Spallation Source [1] (ESS) in Lund (Sweden) will provide the most brilliant neutron beams worldwide. To make efficient use of this source, it is necessary to provide different sample environments with which the potential of the ESS can be exploited as soon as possible from the start of operation. Accordingly, in our opinion, now is the right time to construct and build the sample environments with the construction of “Day 1” instruments [2]. For this purpose, the expertise of three university-based groups from the field of polymer and colloid research was bundled with construction teams of the SKADI [3] and the LOKI [4] instrument and also with the sample environment group of the ESS. Three different “Day 1” sample environments were developed that use a common universal carrier system. This system was intended to enable maximum flexibility with

minimal downtime caused by changing the sample environment. In addition, it should be possible to partially automate the conversion, at least in perspective, since higher radiation is to be expected at the sample location. The following three sample environments were developed as part of the joint project:

- Environment for in situ dynamic light scattering (DLS) combined with small angle neutron scattering;
- Environment for small-angle neutron scattering under grazing incidence (GISANS) [5];
- Environment for neutron scattering on foams [6].

In the first expansion step, these sample environments are to be used on ESS instruments that are optimized for elastic small angle neutron scattering (SANS) for volume samples and GISANS and reflectometry on interface samples. The necessary tests during the development phase were carried out on instruments from the MLZ (Heinz Maier-Leibnitz Zentrum) such as KWS-1 [7] and REFSANS [8]. An innovative concept for a modular sample geometry for the ESS was developed and technically implemented. In particular, the specific demands at the ESS are included in the planning.

In the project, the common model systems used to benchmark all sample environments are so-called smart microgels which are particles with tunable interaction potential. They are called “smart” due to their ability to respond to external stimuli leading to a steadily increasing number of studies dealing with these fascinating materials [9]. The major scientific question of this collaborative research endeavor addresses the interactions of these soft deformable particles in the volume phase and at interfaces. This is extremely important both with regard to the fundamental understanding of the interactions between the particles [10,11] and for the transfer to the life sciences, as well as for technical applications in new technologies [12–15].

The present work focuses on the sample environment for in situ dynamic light scattering (DLS) measurements in combination with small angle neutron scattering. SANS is a valuable method for the investigation of soft matter. Due to the high sensitivity of SANS for organic samples compared to X-ray scattering and the possibility to selectively set the contrast of the molecular species by selecting the isotopic composition of samples and solvent (so-called contrast matching), it is an extremely valuable method in many soft matter fields like studies of self-assembly [16,17], polymer melts [18,19], colloidal polymers such as microgels [20–27], micelles [28,29] and bio-macromolecules like proteins [30,31] or vesicles from lipids [17,32]. Due to the relatively low intensity of neutron beams, often rather long measurements, e.g. compared to light scattering are required to gain data of high quality.

Due to the combination of long measurements and irradiation with neutrons, a stable sample is not always guaranteed. Biological samples might be especially prone to degradation. Therefore, monitoring the sample stability during extended measurements with in situ DLS has recently gained popularity [33–37]. In this work, the components of the sample environment designed for the simultaneous measurement of SANS and DLS at the ESS with a focus on portability and the accommodation of many samples are presented (Section 2). A detailed description of the complete setup, the control software layout and the DLS data analysis can be found in the Section 3.

2. Sample Environment Components

In light of the high-intensity neutron source ESS, our setup features a sample changer for up to 39 samples with three individually temperature controlled compartments.

2.1. Sample Rack/Sample Magazines

The sample rack (Figure 1) holds three magazines for up to 13 standard 1 mm cuvettes (external dimensions: 52 mm · 12.5 mm · 3.5 mm) each. The cuvettes can be flushed with dried air to prevent condensation when measuring at low temperatures. Each of the magazines has a separate connector (CBI, Stäubli, Pfäffikon, Switzerland) for temperature control fluid and is insulated with PEEK, so that three individual temperatures can be

used simultaneously, provided enough thermostats are present. Within each magazine, three positions can be equipped with in-cell Pt-100 thermometers (P0K1.161.2K.Y.5000-4.S, Innovative Sensor Technology IST AG, Ebnat-Kappel, Schweiz). The remaining cuvette temperatures can then be interpolated. The Pt-100 thermometers are read out with a temperature monitor (Model 224, Lake Shore Cryotronics, Westerville, OH, USA). The sample holder temperature is controlled with fluid pumped by a thermostat (FP50-HL, Julabo, Seelbach, Germany).

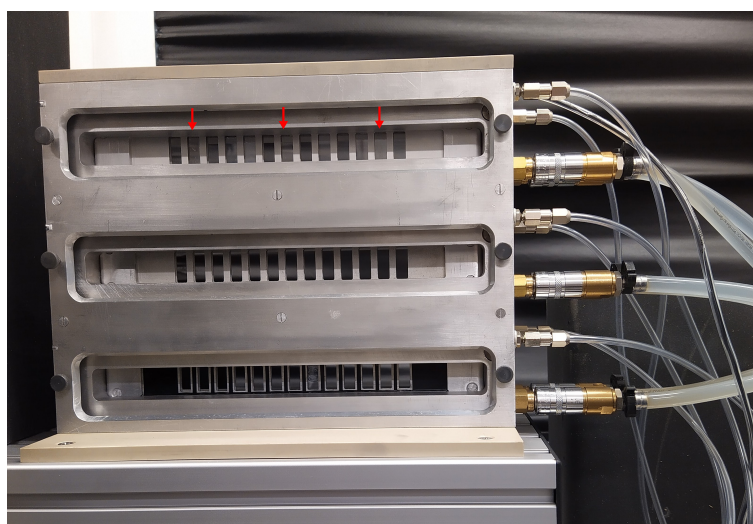


Figure 1. Photograph of the sample changer. The sample changer consists of a rack for 3 magazines each holding up to 13 cuvettes. Each magazine's temperature can be controlled individually. The open sides can be flushed with dried air to prevent condensation, when measuring at low temperatures. This part of the setup can also be used for standard SANS experiments without DLS. The red arrows indicate the cuvette positions, that were used for the temperature measurements in Figure 2.

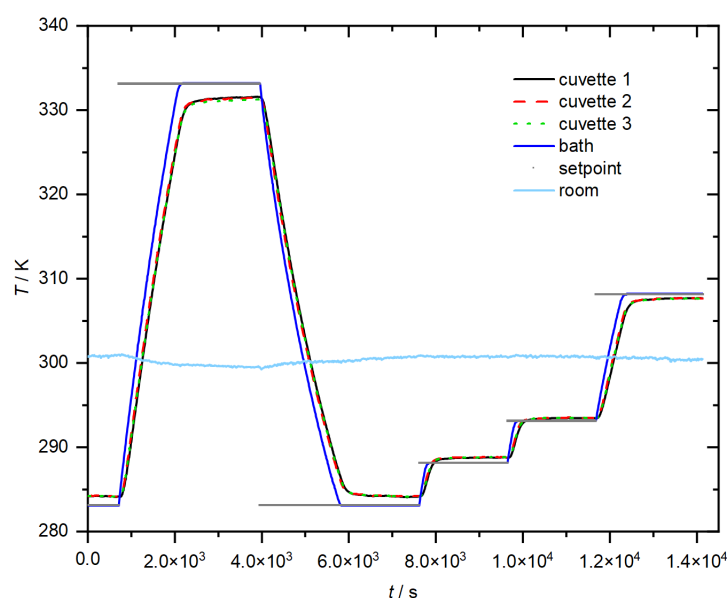


Figure 2. Comparison of set-point temperature, bath temperature and the temperature in three different cuvettes inside the sample holder plotted against time.

The sample aperture is 9 mm · 20 mm for the incident beam and 10 mm · 25 mm on the back. The largest scattering angle possible with this sample environment is 42.5° in the vertical direction. However, it should be noted that the possible scattering angle also depends on the actual configuration of the SANS instruments, e.g., the neutron spot size. However, the sample-to-aperture distance will be a compromise to allow for the incident light to reach the sample cells. The sample environment can be moved along the Y- and Z-axis (in the instrument coordinate system) to change the sample in the neutron beam and laser focus. This is accomplished with two linear translation stages (LS-180, Physik Instrumente, Karlsruhe, Germany).

Temperature Control

Precise and reproducible temperature control is an important issue when working with soft matter samples, due to the influence on molecular interactions and the sample structure. Therefore, the sample holder constructed for this instrument is characterized regarding the temperature control capabilities. The sample environment's temperature can be controlled with various fluids, allowing a temperature range from 253.15 K to 393.15 K, depending on the chosen fluid.

An example of the temperature control characteristics is shown in Figure 2. Here, the set-point temperature, the bath temperature and the temperatures in three different cuvettes filled with water in one magazine (see Figure 1) are plotted against the time. It can be seen that the cuvette temperatures follow the bath temperature rapidly. The cuvette temperatures reach 1 K of their equilibrium temperatures after 1 min and 0.1 K of the equilibrium temperature within 3 min after the bath reached the setpoint temperature even for large temperature steps (50 K). The thermostat takes ca. 30 min to reach the setpoint for cooling 50 K from 333.1 K to 283.1 K. Heating from 283.1 K to 333.1 K takes 23 min. However, smaller temperature steps, from 283.1 K to 288.1 K only take 3 min. These times are dependent on the thermostat used and are only valid for the thermostat (FP50-HL, Julabo, Seelbach, Germany) applied here.

The sample temperature can be measured using a PT-100 thermometer inside three cuvettes for each magazine. Figure 2 shows that all three cuvette temperatures are nearly identical. This indicates a homogeneous temperature distribution for all samples in one magazine. However, to correct even for these slight deviations, the sample temperature for all other cuvettes can be interpolated from the three measured temperatures in each magazine.

2.2. Light Scattering

Dynamic light scattering is a well established method for the characterization of particles in suspension by probing their diffusive behavior [38].

For the dynamic light scattering setup inspired by [36,37], the light scattering plane is inclined by 20° relative to the SANS plane, to prevent problems arising from reflections on the cuvettes. A scheme of the optical setup can be found in Figure 3.

The laser light (633 nm, 21 mW, HNL210L-EC, Thorlabs, Newton, NJ, USA) passes a shutter (SH05/M, Thorlabs, Newton, NJ, USA) and a filter wheel (FW212C, Thorlabs, Newton, NJ, USA) equipped with neutral density filters with optical densities of 0.1, 0.2, 0.3, 0.4, 0.5, 0.6, 1.0, 1.3, 2.0 and 3.0 and is coupled into a polarization-maintaining single mode fiber (P3-630PM-FC-1, Thorlabs, Newton, NJ, USA) with a fiber port (PAF-X-5-A, Thorlabs, Newton, NJ, USA). The laser light is emitted from a fiber collimator (60FC-4-M5-33, Schäfter and Kirchhoff, Hamburg, Germany) and focused onto the sample through a Glan-Thompson polarizer (GTH10M-A, Thorlabs, Newton, NJ, USA). After passing another Glan-Thompson polarizer and a laser line filter (FL632.8-1, Thorlabs, Newton, NJ, USA) the light scattered by the sample is collected by the same collimator type and coupled into a single mode optical fiber (630HP with FC/PC and FC/APC connectors, Thorlabs, Newton, NJ, USA). For the detection in pseudo-cross configuration, a fiber optic beam splitter (ALV, Langen, Germany) is used to split the scattered light in a ratio of about 50:50.

Afterwards, the light is detected into two single photon counting modules (SPCM-AQRH-14-FC, Excelitas Technologies, Waltham, MA, USA). For correlation, a field programmable gate array board (Spartan-6 FPGA, Xilinx, San José, CA, USA) is programmed analogously to a previous implementation for fluorescence correlation spectroscopy [39]. For the alignment of the setup, at first the incident laser beam is focused on the sample position. Then, an auxiliary laser is coupled into the fiber couplers of the detection side, to enable a prealignment by eye. After that, the detection can be easily adjusted to maximum scattered intensity and the quality of the correlation function.

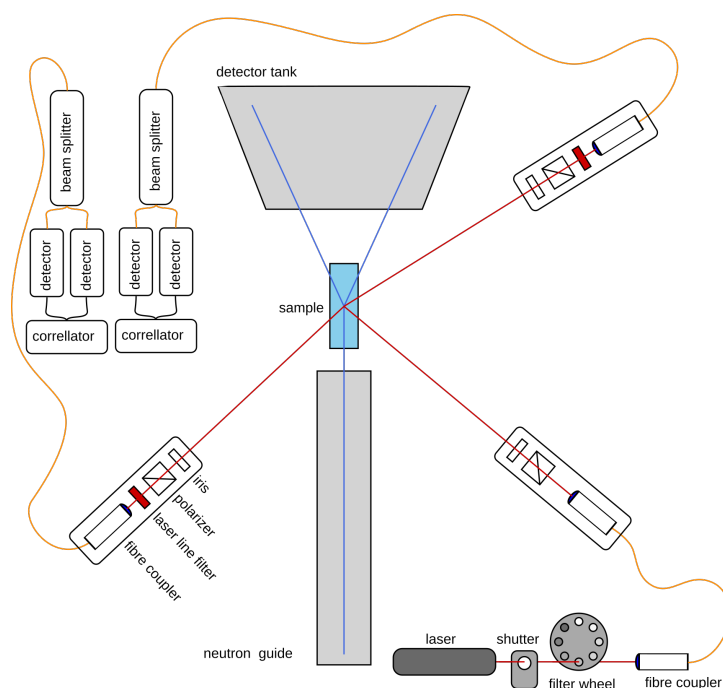


Figure 3. Scheme of the instrument components required for light scattering and the resulting beampath.

The sample environment for in situ dynamic light scattering and SANS measurements is equipped with two parallel setups for measuring dynamic light scattering at two different scattering angles θ of approximately 120° and 71° . Due to refraction on the cuvette–air and cuvette–solvent interfaces, the precise scattering angle is calculated using the refractive index n of the solvent according to Snell’s law for each temperature.

To validate the correct operation of the dynamic light scattering setup, polystyrene standard spheres with a radius of 25 nm and 200 nm were measured. Figure 4 shows a autocorrelation function and the respective cumulant fit for each angle of measurement as an example. Here, sound autocorrelation functions with an intercept of about 1 indicate a well-adjusted light scattering setup. The measurement of an autocorrelation function is completed within 30 s. This enables multiple DLS experiments within the duration of a SANS experiment (some 10 min) and therefore the in situ monitoring of the sample stability.

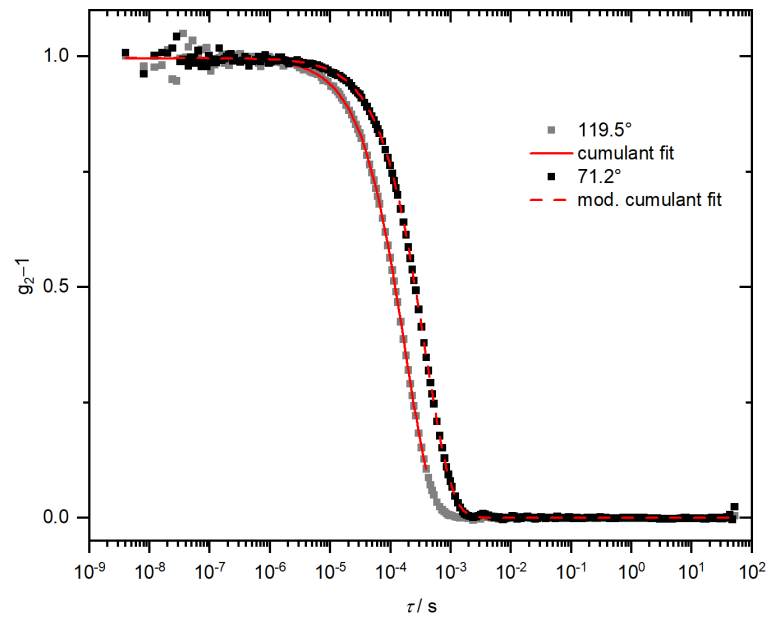


Figure 4. Two correlation functions measured simultaneously at both detection angles. The sample used here was a diluted 50 nm (diameter) polystyrene-sphere standard in H₂O at a temperature of 10.5 °C.

The relaxations rates Γ received from the fit can be converted into the translational diffusion coefficient D_T with the magnitude of the scattering vector $q = \frac{4\pi n}{\lambda} \sin(\frac{\Theta}{2})$. Here, λ is the wavelength, Θ is the scattering angle and n is the refractive index of the solvent.

$$D_T = \frac{\Gamma}{q^2} \quad (1)$$

Then, the hydrodynamic radius R_H is calculated with the Boltzmann constant k_b , the solvent viscosity [40] η and the temperature T using the Stokes–Einstein equation:

$$R_H = \frac{k_b T}{6\pi\eta D_T}. \quad (2)$$

The hydrodynamic radii calculated this way for the particles are shown in Table 1. The measured hydrodynamic radii are consistently slightly bigger than the nominal particle size as indicated by the producer of the standard. This is a common effect in dynamic light scattering and can be attributed to the interaction of the particles with the solvent H₂O and maybe attractive interactions. These values are well in accordance with the measurements performed on these particles with other light scattering setups in our lab.

Table 1. Results of the dynamic light scattering measurements using two different polystyrene latex standards diluted in water with nominal radii of 25 nm and 200 nm, respectively.

	25 nm	200 nm
71°	29.9 ± 0.1 nm	209 ± 6 nm
120°	28.5 ± 0.2 nm	215 ± 3 nm

To test the dynamic light scattering setup at different temperatures, microgels are a suitable and interesting model system, due to the temperature-dependent swelling behavior. Figure 5 shows the swelling behavior of a poly *N*-isopropylmethacrylamide (NIPMAM) microgel crosslinked with the molecule *N,N'*-methylenebisacrylamide. The data were

measured at both angles using the SANS/DLS sample environment. The fully swollen microgel at 12 °C exhibits a hydrodynamic radius of 150 nm. With increasing temperature, the hydrodynamic radius decreases—at first continuously, then drastically from 132 nm at 39 °C to 83 nm at 50 °C with the typical volume phase transition temperature of 45 °C for NIPMAM microgels. Within the experimental precision, the results agree perfectly with previous measurements on commercial DLS machines [26,27]. To further illustrate this agreement, Figure 5, right, shows the correlation functions of the NIPMAM microgel measured at 56 °C with the SANS/DLS setup compared to correlation functions obtained at the same q -values with a commercial setup (ALV GmbH, Langen, Germany) equipped with a Nd:YAG-laser ($\lambda = 532$ nm). The data are in excellent agreement. Moreover, no compressed exponential decays were observed for the microgel samples measured here, pointing to the absence of convection [41].

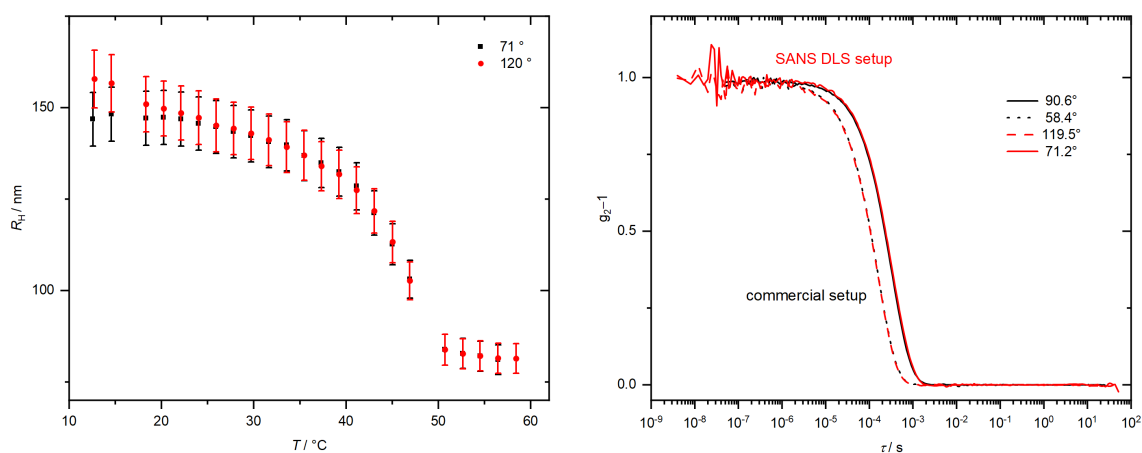


Figure 5. (left): Swelling behavior of a NIPMAM microgel measured with the SANS/DLS setup at both scattering angles. (right): comparison of autocorrelation functions of the NIPMAM microgel at 56 °C for both angles (red) compared to ACFs measured with a commercial ALV setup (black curves, measured with a different laser wavelength and therefore at different angles to achieve the same q value) at the same q -values of 0.23 nm^{-1} and 0.15 nm^{-1} .

2.3. SANS Measurements

To validate the sample environment design for SANS measurements, tests were performed at the MLZ. A sample was measured in the newly constructed sample environment and compared to neutron data previously recorded using the D11 SANS machine at the Institute Laue Langevin (ILL). Figure 6 shows the results of a measurement using the sample holder introduced in this work at the KWS-1 [7] SANS instrument at the MLZ. Figure 6, top, shows a comparison of measurements of the same NIPMAM microgel as investigated in Figure 5, performed as the reference at the ILL using the instrument D11 and with the new sample environment at MLZ. The scattering curves show a satisfactory agreement. The slight deviation at low q can be attributed to resolution effects.

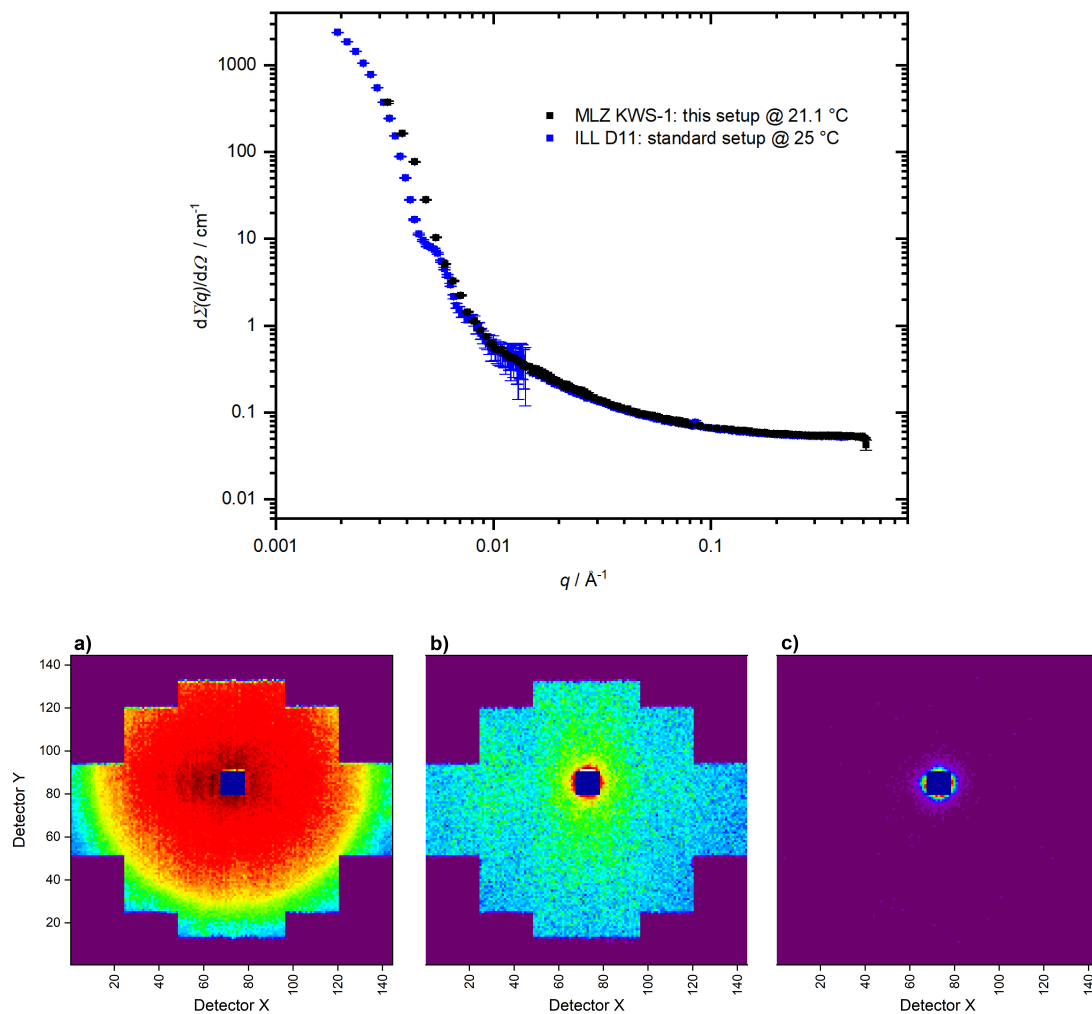


Figure 6. (top): SANS data measured employing the new sample environment from this work using the KWS1 machine at MLZ compared to SANS measurements made with the ILL standard setup at the D11 instrument. For both measurements, the same NIPMAM microgel sample as for the DLS measurements was used. **(bottom):** detector images for an empty cell measurement at 2 m (a), 5 m (b) and 20 m (c). The reflections seen here, are caused by the large distance between the nose of the collimation system and the sample cells.

Figure 6, bottom, shows detector images of empty-cell measurements at 2 m, 5 m and 20 m sample–detector distances. Especially for the detector image of the 5 m measurement, an inhomogeneous scattering can be observed. This behavior is attributed to reflections on the sample holder and the walls of the cuvettes which is caused by the rather large distance between the final window of the collimation system and the sample cells and the not fully adapted collimation. This large distance is due to spatial constraints of the sample environment which was not optimized for the KWS-1 machine.

Furthermore, a rather strong background scattering can be observed. This is also due to the relatively long air path which we had to take in the test measurements. This causes the increased background scattering. However, this will not be a problem for the instruments SKADI and LOKI at ESS, due to the optimization of the sample environment for these SANS instruments.

3. The Fully Assembled Sample Environment

3.1. General Remarks

The in situ SANS/DLS instrument setup was designed with portability and modularity in mind, to guarantee the compatibility with various SANS instruments at the ESS and to enable a fast change of sample environments with only minimal work necessary. For the portability of the setup, all equipment and electronics needed for the light scattering measurements were mounted in 19 inch racks inside a box. This box is constructed from aluminum profiles (Rose und Krieger, Minden, Germany) and fits into the footprint of a EUR-pallet. A photograph of the complete setup can be seen in Figure 7. As versatile interface a 120 cm · 90 cm breadboard (M-SG-34-2, Newport, CA, USA) is mounted on top of the aluminum box. The breadboard is screwed down on the aluminum box to prevent the shifting of the optical setup and to guarantee a stable transport of the complete setup e.g., by forklift or crane. For transport using a crane, a crane eye is installed on each edge of the box. This base construction is identical for all FlexiProb sample environments and can be easily moved to the instrument cave using a pallet jack.

The setup is constructed, so that it can be put into operation with only a few connections made. Power is supplied by a single 32 A IEC 60309 plug. The thermostat cycle needs to be connected and the RS232-cable needs to be connected to the thermostat. Further pressurized dried air, the laser interlock and an Ethernet connection are required for operation. The patch panel layout of the setup is suitable for connectors available at ESS instruments such as SKADI and LOKI.

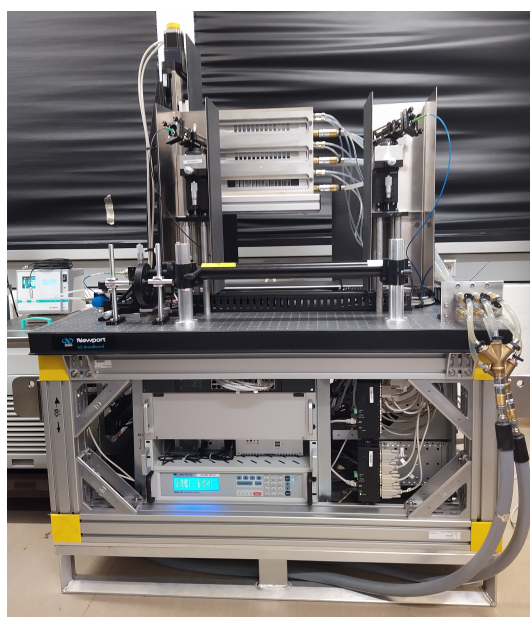


Figure 7. Photograph of the complete SANS/DLS setup with carrier structure.

The general architecture of the interacting systems is described in the scheme in Figure 8. The user interacts with the setup either via the networked instrument control system (NICOS) [42,43] client or the DLS-GUI program, for direct control of the data fits. The measurement is controlled by the NICOS server, where the single NICOS devices can communicate with the input output controllers (IOCs) in the experimental physics and industrial control system (EPICS) [44] server. From the EPICS server, the hardware devices are controlled via their respective protocols, namely USB, Ethernet, an Ethernet-to-RS232-converter (EX-6034, EXSYS, Steinbach, Germany) or by the direct control of the power supply with switchable power outlets (Multibox, ANTRAX Datentechnik, Herford, Germany).

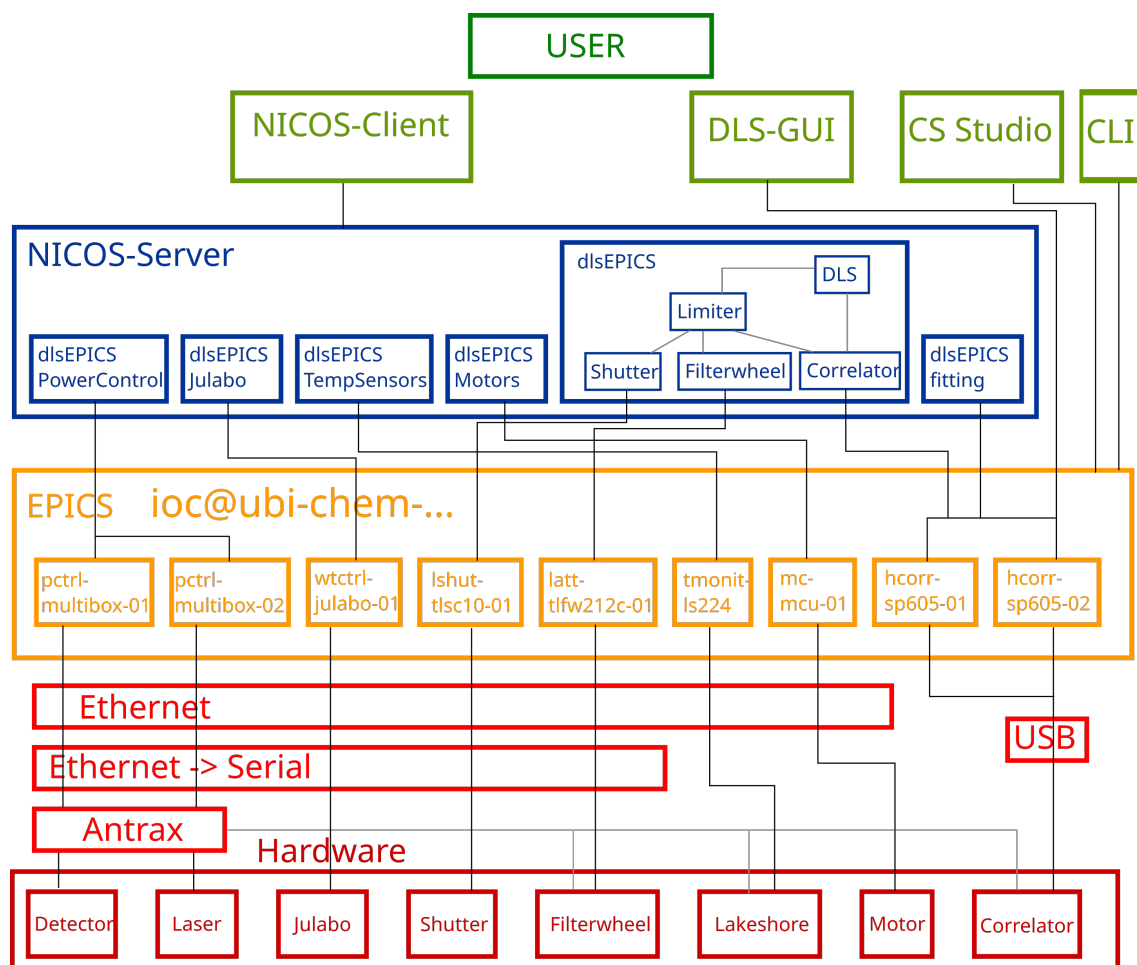


Figure 8. Schematic representation of the architecture of the setup. The user can interact via the NICOS client with the NICOS server [42,43], where the measurements are controlled. Low level-control of the devices is implemented via EPICS, that is connected via different protocols to the hardware. Alternatively, the EPICS process variables can be directly manipulated via the program CS Studio or the command line interface (CLI).

3.1.1. Safety Precautions

For laser safety, a shutter is installed in the setup. The shutter interlock will be connected to the instruments' safety environments' doors, so that no laser radiation can escape during operation. To prevent laser reflexes from the sample holder and physical contact with the cadmium, the Cd-mask in the sample holder is covered by a black polymer film. To prevent the activation of the sample environment from the neutron radiation, the sample rack and magazines are constructed from aluminum, polyether ether ketone (PEEK), and titanium screws. Boron-based neutron shielding (5 mm Mirrobor, Mirrotron, Budapest, Hungary) is applied to avert activation of the sample environment from neutron reflexes originating from the sample. For this, shielding is mounted on the side of the sample holder facing the axis of the translation unit and below the sample holder. As the optical setup could not be realized using only neutron-compatible materials, neutron shielding is also applied around the three optical towers used for light scattering.

3.1.2. Automated Data Analysis

For the analysis of the autocorrelation functions, three methods were implemented in the software. The data can be evaluated during the measurement using inverse Laplace transformation by means of the program CONTIN [45]. Moreover, the standard version of the method of cumulants [46] can be used for fits of the region of short correlation times or a modified method of cumulants can be used for larger times [47,48]. This way, the relaxation

rate Γ and accordingly, the sample size and stability, can be monitored on-line during the SANS measurement.

Figure 9 shows the GUI of a custom program developed to monitor the measurements and fits during the runtime. Shown is the auto correlation function, the intensity trace (top row), the residuals from the fit and the resulting gamma distribution function (bottom row). This program bypasses the NICOS-server and receives the data directly from the correlators. Therefore, custom fits can also be tried out locally before modifying the settings for the automated fitting. Hence, the sample can be characterized in situ and deterioration can be detected during the course of the SANS measurements.



Figure 9. Application for controlling and monitoring the fits of the data during the measurements.

4. Conclusions

A new sample environment for in situ dynamic light scattering and SANS at the ESS was developed. The entire setup was transferred to MLZ and test measurements were performed. The sample environment was used to successfully measure SANS. The background problem will be solved at the ESS using a smaller distance between the individual sample cells and the end window of the collimation system. The simultaneous operation of the DLS system was proven for both configured scattering angles. The sample environments' capabilities regarding temperature control and measurement were also characterized and fulfill all specifications. The integration of all devices in both EPICS and NICOS was successfully finished, making the sample environment ready for integration and first tests at the ESS.

Author Contributions: Conceptualization, T.H., P.M.-B. and R.v.K.; SANS measurements, A.J.S. and H.F.; software, A.J.S., G.B., T.B. and L.W.; construction of the light scattering setup, A.J.S. and L.W.; construction of the carrier system: A.J.S., S.J., J.R., H.S., A.H., T.B., T.W., L.P.K., M.K., O.L. and L.W.; writing—original draft preparation, L.W. and T.H.; writing—review and editing, A.J.S., S.J., H.S., A.H., T.B., T.H., T.W., J.R., L.P.K., M.K., H.F., O.L., P.M.-B., R.v.K.; visualization, L.W.; supervision, T.H.; project administration, T.H.; funding acquisition, T.H., P.M.-B. and R.v.K. All authors have read and agreed to the published version of the manuscript.

Funding: This research was funded by the German Federal Ministry for Education and Research (BMBF) within the project “FlexiProb” sample environment grant number 05K2016.

Institutional Review Board Statement: Not applicable.

Informed Consent Statement: Not applicable.

Data Availability Statement: The data shown is available on request from the corresponding author.

Acknowledgments: We gratefully acknowledge the ESS Motion Control Group for help implementing the control of the translation stage. We gratefully acknowledge Tobias Schrader for varied fruitful discussions, Yvonne Hannapel and Simon Staringer for help during the SANS test experiments. Furthermore, we thank Claus Seidel (HHU, Düsseldorf) for the original version of the software used to operate the FPGA as a correlator. We gratefully acknowledge financial support for the publication costs by the Open Access Publication Fund of Bielefeld University.

Conflicts of Interest: The authors declare no conflict of interest.

References

1. Garoby, R.; Vergara, A.; Danared, H.; Alonso, I.; Bargallo, E.; Cheymol, B.; Darve, C.; Eshraqi, M.; Hassanzadegan, H.; Jansson, A.; et al. The European Spallation Source Design. *Phys. Scr.* **2017**, *93*, 014001. [[CrossRef](#)]
2. Andersen, K.; Argyriou, D.; Jackson, A.; Houston, J.; Henry, P.; Deen, P.; Toft-Petersen, R.; Beran, P.; Strobl, M.; Arnold, T.; et al. The instrument suite of the European Spallation Source. *Nucl. Instrum. Methods Phys. Res. Sect. A Accel. Spectrometers Detect. Assoc. Equip.* **2020**, *957*, 163402. [[CrossRef](#)]
3. Frielinghaus, P.H. *ESS Instrument Construction Proposal SKADI*; ESS: Lund, Sweden, 2017.
4. Jackson, A.J.; Kanaki, K. *ESS Construction Proposal LOKI—A Broad-Band SANS Instrument*; ESS: Lund, Sweden, 2013.
5. Widmann, T.; Kreuzer, L.P.; Kühnhammer, M.; Löhmann, O.; Schmid, A.J.; Wiehemeier, L.; Jaksch, S.; Frielinghaus, H.; Schneider, H.; Hiess, A.; et al. Flexible sample environment for the investigation of soft matter at the European Spallation Source: Part II—The GISANS setup. *Appl. Sci.* **2021**, *11*, 4036.
6. Kühnhammer, M.; Widmann, T.; Kreuzer, L.; Schmid, A.J.; Wiehemeier, L.; Frielinghaus, H.; Jaksch, S.; Bögershausen, T.; Barron, P.; Schneider, H.; et al. Flexible sample environments for the investigation of soft matter at the European Spallation Source: Part III—The macroscopic foam cell. *Appl. Sci.* **2021**, to be submitted.
7. Feoktystov, A.V.; Frielinghaus, H.; Di, Z.; Jaksch, S.; Pipich, V.; Appavou, M.S.; Babcock, E.; Hanslik, R.; Engels, R.; Kemmerling, G.; et al. KWS-1 high-resolution small-angle neutron scattering instrument at JCNS: Current state. *J. Appl. Crystallogr.* **2015**, *48*, 61–70. [[CrossRef](#)]
8. Moulin, J.F.; Haese, M. REFSANS: Reflectometer and evanescent wave small angle neutron spectrometer. *J. Large-Scale Res. Facil. JLSRF* **2015**, *1*, 9. [[CrossRef](#)]
9. Karg, M.; Pich, A.; Hellweg, T.; Hoare, T.; Lyon, L.A.; Crassous, J.J.; Suzuki, D.; Gumerov, R.A.; Schneider, S.; Potemkin, I.I.; et al. Nanogels and microgels: From model colloids to applications, recent developments, and future trends. *Langmuir* **2019**, *35*, 6231–6255. [[CrossRef](#)]
10. Scotti, A.; Denton, A.R.; Brugnoli, M.; Houston, J.E.; Schweins, R.; Potemkin, I.I.; Richtering, W. Deswelling of microgels in crowded suspensions depends on cross-link density and architecture. *Macromolecules* **2019**, *52*, 3995–4007. [[CrossRef](#)]
11. Mohanty, P.S.; Nöjd, S.; van Gruijthuijsen, K.; Crassous, J.J.; Obiols-Rabasa, M.; Schweins, R.; Stradner, A.; Schurtenberger, P. Interpenetration of polymeric microgels at ultrahigh densities. *Sci. Rep.* **2017**, *7*, 1–12. [[CrossRef](#)] [[PubMed](#)]
12. Lyon, L.A.; Meng, Z.; Singh, N.; Sorrell, C.D.; John, A.S. Thermoresponsive microgel-based materials. *Chem. Soc. Rev.* **2009**, *38*, 865. [[CrossRef](#)]
13. Menne, D.; Pitsch, F.; Wong, J.E.; Pich, A.; Wessling, M. Temperature-modulated water filtration using microgel-functionalized hollow-fiber membranes. *Angew. Chem. Int. Ed.* **2014**, *53*, 5706–5710. [[CrossRef](#)] [[PubMed](#)]
14. Uhlig, K.; Wegener, T.; He, J.; Zeiser, M.; Bookhold, J.; Dewald, I.; Godino, N.; Jaeger, M.; Hellweg, T.; Fery, A.; et al. Patterned thermoresponsive microgel coatings for noninvasive processing of adherent cells. *Biomacromolecules* **2016**, *17*, 1110–1116. [[CrossRef](#)] [[PubMed](#)]
15. Bookhold, J.; Dirksen, M.; Wiehemeier, L.; Knust, S.; Anselmetti, D.; Paneff, F.; Zhang, X.; Gölzhäuser, A.; Kottke, T.; Hellweg, T. Smart membranes by electron beam cross-linking of copolymer microgels. *Soft Matter* **2021**, *17*, 2205–2214. [[CrossRef](#)] [[PubMed](#)]
16. Bergström, M.; Pedersen, J.S.; Schurtenberger, P.; Egelhaaf, S.U. Small-angle neutron scattering (SANS) study of vesicles and lamellar sheets formed from mixtures of an anionic and a cationic surfactant. *J. Phys. Chem. B* **1999**, *103*, 9888–9897. [[CrossRef](#)]
17. Dargel, C.; Geisler, R.; Hannappel, Y.; Kemker, I.; Sewald, N.; Hellweg, T. Self-assembly of the bio-surfactant aescin in solution: A small-angle x-ray scattering and fluorescence study. *Colloids Interfaces* **2019**, *3*, 47. [[CrossRef](#)]
18. Muller, R.; Pesce, J.J.; Picot, C. Chain conformation in sheared polymer melts as revealed by SANS. *Macromolecules* **1993**, *26*, 4356–4362. [[CrossRef](#)]
19. Hammouda, B. SANS from homogeneous polymer mixtures: A unified overview. In *Advances in Polymer Science*; Springer: Berlin/Heidelberg, Germany, 1993; pp. 87–133. [[CrossRef](#)]
20. Tennenbaum, M.; Anderson, C.; Hyatt, J.S.; Do, C.; Fernandez-Nieves, A. Internal structure of ultralow-crosslinked microgels: From uniform deswelling to phase separation. *Phys. Rev. E* **2021**, *103*, 022614. [[CrossRef](#)]
21. Widmann, T.; Kreuzer, L.P.; Hohn, N.; Bießmann, L.; Wang, K.; Rinner, S.; Moulin, J.F.; Schmid, A.J.; Hannappel, Y.; Wrede, O.; et al. Hydration and Solvent Exchange Induced Swelling and Deswelling of Homogeneous Poly(N-isopropylacrylamide) Microgel Thin Films. *Langmuir* **2019**, *35*, 16341–16352. [[CrossRef](#)] [[PubMed](#)]
22. Virtanen, O.L.J.; Kather, M.; Meyer-Kirschner, J.; Melle, A.; Radulescu, A.; Viell, J.; Mitsos, A.; Pich, A.; Richtering, W. Direct monitoring of microgel formation during precipitation polymerization of N-isopropylacrylamide using in situ SANS. *ACS Omega* **2019**, *4*, 3690–3699. [[CrossRef](#)]

23. Cors, M.; Wiehemeier, L.; Hertle, Y.; Feoktystov, A.; Cousin, F.; Hellweg, T.; Oberdisse, J. Determination of internal density profiles of smart acrylamide-based microgels by small-angle neutron scattering: A multishell reverse Monte Carlo approach. *Langmuir* **2018**, *34*, 15403–15415. [[CrossRef](#)]
24. Stieger, M.; Pedersen, J.S.; Lindner, P.; Richtering, W. Are thermoresponsive microgels model systems for concentrated colloidal suspensions? A rheology and small-angle neutron scattering study. *Langmuir* **2004**, *20*, 7283–7292. [[CrossRef](#)] [[PubMed](#)]
25. Crowther, H.M.; Saunders, B.R.; Mears, S.J.; Cosgrove, T.; Vincent, B.; King, S.M.; Yu, G.E. Poly(NIPAM) microgel particle de-swelling: A light scattering and small-angle neutron scattering study. *Colloids Surfaces A Physicochem. Eng. Asp.* **1999**, *152*, 327–333. [[CrossRef](#)]
26. Wedel, B.; Zeiser, M.; Hellweg, T. Non NIPAM based smart microgels: Systematic variation of the volume phase transition temperature by copolymerization. *Z. Phys. Chem.* **2012**, *226*, 737–748. [[CrossRef](#)]
27. Wiehemeier, L.; Cors, M.; Wrede, O.; Oberdisse, J.; Hellweg, T.; Kottke, T. Swelling behaviour of core-shell microgels in H₂O, analysed by temperature-dependent FTIR spectroscopy. *Phys. Chem. Chem. Phys.* **2019**, *21*, 572–580. [[CrossRef](#)]
28. Sochor, B.; Düdükü, Ö.; Lübtow, M.M.; Schummer, B.; Jaksch, S.; Luxenhofer, R. Probing the complex loading-dependent structural changes in ultrahigh drug-loaded polymer micelles by small-angle neutron scattering. *Langmuir* **2020**, *36*, 3494–3503. [[CrossRef](#)] [[PubMed](#)]
29. Hayter, J.B. Neutron scattering from concentrated micellar solutions. *Berichte Bunsenges. Phys. Chem.* **1981**, *85*, 887–891. [[CrossRef](#)]
30. Svergun, D.I.; Richard, S.; Koch, M.H.J.; Sayers, Z.; Kuprin, S.; Zaccai, G. Protein hydration in solution: Experimental observation by x-ray and neutron scattering. *Proc. Natl. Acad. Sci. USA* **1998**, *95*, 2267–2272. [[CrossRef](#)]
31. Cousin, F.; Gummel, J.; Ung, D.; Boué, F. Polyelectrolyte-protein complexes: Structure and conformation of each specie revealed by SANS. *Langmuir* **2005**, *21*, 9675–9688. [[CrossRef](#)]
32. Sreij, R.; Dargel, C.; Geisler, P.; Hertle, Y.; Radulescu, A.; Pasini, S.; Perez, J.; Moleiro, L.H.; Hellweg, T. DMPC vesicle structure and dynamics in the presence of low amounts of the saponin aescin. *Phys. Chem. Chem. Phys.* **2018**, *20*, 9070–9083. [[CrossRef](#)]
33. Nigro, V.; Angelini, R.; King, S.; Franco, S.; Buratti, E.; Bomboi, F.; Mahmoudi, N.; Corvasce, F.; Scaccia, R.; Church, A.; et al. Apparatus for simultaneous dynamic light scattering–small angle neutron scattering investigations of dynamics and structure in soft matter. *Rev. Sci. Instrum.* **2021**, *92*, 023907. [[CrossRef](#)]
34. Nawroth, T.; Buch, P.; Buch, K.; Langguth, P.; Schweins, R. Liposome formation from bile salt–lipid micelles in the digestion and drug delivery model FaSSIFmod estimated by combined time-resolved neutron and dynamic light scattering. *Mol. Pharm.* **2011**, *8*, 2162–2172. [[CrossRef](#)] [[PubMed](#)]
35. Balacescu, L.; Vögl, F.; Staringer, S.; Ossovyi, V.; Brandl, G.; Lumma, N.; Feilbach, H.; Holderer, O.; Pasini, S.; Stadler, A.; et al. In situ dynamic light scattering complementing neutron spin-echo measurements on protein samples. *J. Surf. Investig. X-Ray Synchrotron Neutron Tech.* **2020**, *14*, S185–S189. [[CrossRef](#)]
36. Kohlbrecher, J.; Bollhalder, A.; Vavrin, R.; Meier, G. A high pressure cell for small angle neutron scattering up to 500 MPa in combination with light scattering to investigate liquid samples. *Rev. Sci. Instrum.* **2007**, *78*, 125101. [[CrossRef](#)] [[PubMed](#)]
37. Vavrin, R.; Kohlbrecher, J.; Wilk, A.; Ratajczyk, M.; Lettinga, M.P.; Buitenhuis, J.; Meier, G. Structure and phase diagram of an adhesive colloidal dispersion under high pressure: A small angle neutron scattering, diffusing wave spectroscopy, and light scattering study. *J. Chem. Phys.* **2009**, *130*, 154903. [[CrossRef](#)] [[PubMed](#)]
38. Berne, B.J.; Pecora, R. *Dynamic Light Scattering: With Applications to Chemistry, Biology, and Physics*; Dover Publications Inc.: New York, NY, USA, 2000; ISBN 0486442276.
39. Kalinin, S.; Kühnemuth, R.; Vardanyan, H.; Seidel, C.A.M. Note: A 4 ns hardware photon correlator based on a general-purpose field-programmable gate array development board implemented in a compact setup for fluorescence correlation spectroscopy. *Rev. Sci. Instrum.* **2012**, *83*, 096105. [[CrossRef](#)]
40. Cho, C.H.; Urquidi, J.; Singh, S.; Robinson, G.W. Thermal offset viscosities of liquid H₂O, D₂O, and T₂O. *J. Phys. Chem. B* **1999**, *103*, 1991–1994. [[CrossRef](#)]
41. Gabriel, J.; Blochowicz, T.; Stühn, B. Compressed exponential decays in correlation experiments: The influence of temperature gradients and convection. *J. Chem. Phys.* **2015**, *142*, 104902. [[CrossRef](#)]
42. Brandl, G.; Felder, C.; Pedersen, B.; Faulhaber, E.; Lenz, A.; Krüger, J. NICOS–The Instrument Control solution at the MLZ. In Proceedings of the 10th International Workshop on Personal Computers and Particle Accelerator Controls, Karlsruhe, Germany, 14–17 October 2014; Number IMPULSE-2014-00016.
43. Available online: <https://nicos-controls.org/> (accessed on 29 April 2021).
44. Dalesio, L.R.; Kozubal, A.J.; Kraimer, M.R. *EPICS Architecture*; Los Alamos National Lab.: Los Alamos, NM, USA, 1991.
45. Provencher, S.W. CONTIN: A general purpose constrained regularization program for inverting noisy linear algebraic and integral equations. *Comput. Phys. Commun.* **1982**, *27*, 229–242. [[CrossRef](#)]
46. Koppel, D.E. Analysis of macromolecular polydispersity in intensity correlation spectroscopy: The method of cumulants. *J. Chem. Phys.* **1972**, *57*, 4814–4820. [[CrossRef](#)]
47. Frisken, B.J. Revisiting the method of cumulants for the analysis of dynamic light-scattering data. *Appl. Opt.* **2001**, *40*, 4087. [[CrossRef](#)]
48. Hassan, P.; Kulshreshtha, S. Modification to the cumulant analysis of polydispersity in quasielastic light scattering data. *J. Colloid Interface Sci.* **2006**, *300*, 744–748. [[CrossRef](#)] [[PubMed](#)]